

5-2012

# Study of the fundamental chemical and physical interactions between chitosan and hydroxyapatite

Abigail Washispack

*University of Arkansas, Fayetteville*

Follow this and additional works at: <http://scholarworks.uark.edu/baeguht>

---

## Recommended Citation

Washispack, Abigail, "Study of the fundamental chemical and physical interactions between chitosan and hydroxyapatite" (2012).  
*Biological and Agricultural Engineering Undergraduate Honors Theses*. 29.  
<http://scholarworks.uark.edu/baeguht/29>

This Thesis is brought to you for free and open access by the Biological and Agricultural Engineering at ScholarWorks@UARK. It has been accepted for inclusion in Biological and Agricultural Engineering Undergraduate Honors Theses by an authorized administrator of ScholarWorks@UARK. For more information, please contact [scholar@uark.edu](mailto:scholar@uark.edu).

Confidential

Study of the Fundamental Chemical and Physical Interactions between Chitosan and  
Hydroxyapatite Nanoparticles

An Undergraduate Honors College Thesis

in the

Department of Biological Engineering  
College of Engineering  
University of Arkansas  
Fayetteville, AR

by

Abigail Washispack

April 27<sup>th</sup>, 2012

## **Abstract**

Hydroxyapatite and chitosan are widely used in biomedical applications due to their biocompatibility and biodegradability. Various studies show that composites made of hydroxyapatite and chitosan exhibit desirable properties for applications in bone tissue engineering. When creating a composite it is important to understand the interfacial chemistry and physical interactions between the composite materials. An understanding of these properties gives more insight into the resulting structure of the composite on multiple levels (nano- micro- macro). This structure affects the chemical, physical, and mechanical properties of the material, thus analysis of these properties gives a better understanding of how a material will perform when used in various applications. The goal of this research project was to explore the chemical and physical interactions that occur between hydroxyapatite nanoparticles (HANPs) and the polymer chitosan in a novel nanocomposite.

In this project, composites of HANPs and chitosan were synthesized using varying concentrations of the two materials. The composites were analyzed through particle size analysis, Scanning Electron Microscopy (SEM), Dispersive X-ray spectroscopy (EDX), Nuclear Magnetic Resonance spectroscopy (NMR), and X-ray Diffraction (XRD). The results of the study showed mixtures of 10% chitosan and 90% HANPs (dry weight fraction) produce composites with the smallest particle size. The particle size of this composite was then further reduced through chemo-mechanical processing to create a nanocomposite. NMR data suggests that chemical interactions occur between the materials and from analysis of their chemical structures these interactions are most likely hydrogen bonding and coordination bonds. XRD analysis shows a phase change does not occur in the composite after mixing, however there are some phase changes after chemo-mechanical processing.

## **Acknowledgements**

Special thanks to:

Dr. Ajay P. Malshe – for encouraging undergraduates to become involved with research

Dr. Anoop Samant- for continual guidance and support

Wenyang Zhang - for help with particle analysis equipment and XRD analysis

Mourad Benamara – for help in learning SEM imaging

Mike Hawkridge – for expertise in XRD imaging

Parts of this work were financially supported by a Student Undergraduate Research Fellowship grant from the Arkansas Department of Higher Education. Any opinions, findings, and conclusions or recommendations expressed in this material are those of the author and do not necessarily reflect the views of the Arkansas Department of Higher Education.

This thesis is approved.

Thesis Advisor:

A handwritten signature in black ink, appearing to read 'Ajay Malshe', written over a horizontal line.

Dr. Ajay Malshe

Thesis Committee:

---

Dr. Julie Carrier

---

Dr. David Zaharoff

## Table of Contents

|   |    |
|---|----|
| Acknowledgements.....                               | i  |
| Introduction .....                                  | 2  |
| Methods.....  | 6  |
| Composite Preparation .....                         | 6  |
| Chemo-Mechanical Processing .....                   | 7  |
| Results.....  | 7  |
| Particle Size Determination .....                   | 7  |
| Energy Dispersion X-ray Spectroscopy (EDX).....     | 13 |
| Nuclear Magnetic Resonance Spectroscopy (NMR) ..... | 15 |
| X-Ray Diffraction Spectroscopy (XRD) .....          | 17 |
| Discussion.....                                     | 18 |
| Conclusions .....                                   | 19 |
| Future Directions .....                             | 20 |
| References .....                                    | 21 |

## Introduction

The prevalence of patients with bone loss and fracture from various diseases continues to increase in the United States. Among these diseases is osteoporosis, which causes a decrease in bone mineral density [1–3]. Several solutions to the problem of bone loss exist today, including bone autografts and allografts, however both of these treatments have their own disadvantages. Bone autograft complications include insufficient wound healing, donor pain, and insufficient bone material to fill fractures and gaps. Allografts on the other hand pose threats of patient immune reactions and transmissible diseases [4]. Another solution to the problem of bone loss is bone implants made of hydroxyapatite, glass-ceramics, or titanium [5]. In the area of vertebrae bone density loss, injectable polymer methyl methacrylate (PMMA) composites are most common. These composites are normally used in vertebroplasty in which PMMA is injected into a vertebra with decreased bone density or fracture. The use of PMMA in this application however poses various problems. After injection, the polymer's dense nature can lead to subsequent vertebrae compression fractures. Other negative aspects include failure to adhere to surrounding bone surfaces, high exothermic reaction temperature, and insufficient degradation in the body [3].

In recent years mixtures of nanoparticles in different dispersion media have become a common method for drug delivery and tissue repair. In general nanoparticles are preferred in these applications when compared to microparticles because they have distinct properties that can be tuned during synthesis. Nanoparticles also resemble the size of biological molecules (e.g.

proteins, DNA, signal molecules) and structures (e.g. viruses and bacteria), which allows them to better interact with the native, target tissues [6].

Due to the desirable properties of nanoparticles, the goal of this project was to create a composite made of nanoparticles for use in bone tissue repair. This composite would be used in patients by injecting it into areas of bone loss or bone fracture. After creating this composite, the goal was to explore the chemical and physical interactions between the nanoparticles and the dispersion medium. Understanding this interfacial chemistry between the materials gives insight into the resulting nano- micro- macro structure, which affects the physical and chemical properties of material. By understanding these properties, a better understanding is gained of how the material will perform when used in various applications.

There are many kinds of nanoparticles used in different biomedical applications. Examples can be found in Table 1 and of these materials, hydroxyapatite and silica are used in bone tissue applications. Along with these are various materials used as dispersion media to carry the nanoparticles inside the body (Table 2). All of these dispersion media however have various drawbacks for this project.

**Table 1. Nanoparticles for Biomedical Applications**

| <b>Nanoparticle Material</b> | <b>Biomedical Application</b> |
|------------------------------|-------------------------------|
| Hydroxyapatite               | Bone repair/growth [7]        |
| Silica                       | Bone repair/growth [8]        |
| Gold                         | Tumor targeting [9]           |
| Albumin                      | Tumor targeting [10]          |
| Glycol Chitosan              | Low water soluble drugs [11]  |



**Table 2. Common Nanoparticle Dispersion Media**

| <b>Dispersion Medium</b> | <b>Drawbacks</b>  |
|--------------------------|---|
| Methyl Methacrylate      | Low osteoconductivity, cell attachment and proliferation [1,3]                        |
| Alginate Hydrogel        | Preparation time more than 24 hours [12]  |
| Carboxymethyl Chitin     | Difficult to prepare from chitin; commercial sources not economical [13]              |
| Carboxymethyl Chitosan   | Difficult to prepare from chitin and chitosan; commercial sources not economical [14] |

In recent years, hydroxyapatite and chitosan have become common materials used in the area of bone tissue engineering. Composites made of these materials have proved to be more promising for bone repair and replacement when compared to other materials and treatment methods [4].

Hydroxyapatite  $[\text{Ca}_{10}(\text{PO}_4)_6(\text{OH})_2]$  is a major inorganic component of the human body [15,16]. It is known to be biocompatible, bioactive, and has been used successfully in various biomedical applications [13,17–19]. As seen in Figure 1, hydroxyapatite has a hexagonal crystal structure. For pure hydroxyapatite, the calcium phosphate ratio is 1.67 [20]. Pure hydroxyapatite however has poor mechanical properties, including brittleness, and is difficult to mold into a desired shape. Its direct implantation also results in displacement of the material from its intended tissue [12,16]. Thus, hydroxyapatite by itself is a poor biomaterial, despite its positive biological properties.

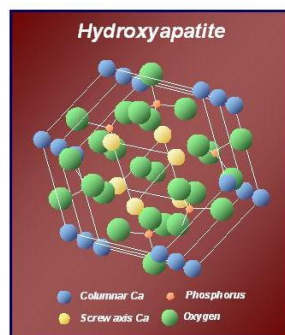


**Figure 1. Crystal Structure of Hydroxyapatite [21]**

Chitosan is biocompatible, non-toxic, biorenewable, and biodegradable [22–24]. It is also known to promote cell growth and has been used in numerous biomedical applications such as wound dressings and drug delivery [14,24]. Chitosan is a linear, heteropolysaccharide consisting of  $\beta$ -1,4-linked glucosamine and N-acetylglucosamine units (Fig. 2). This linkage results in a rigid and unbranched structure. The crystalline structure and presence of hydroxyl groups allow for both intra- and intermolecular hydrogen bonding [24]. In previous studies, chitosan has been used as an adhesive to solve the problem of hydroxyapatite displacement and to allow for molding of hydroxyapatite into a desired shape [23].

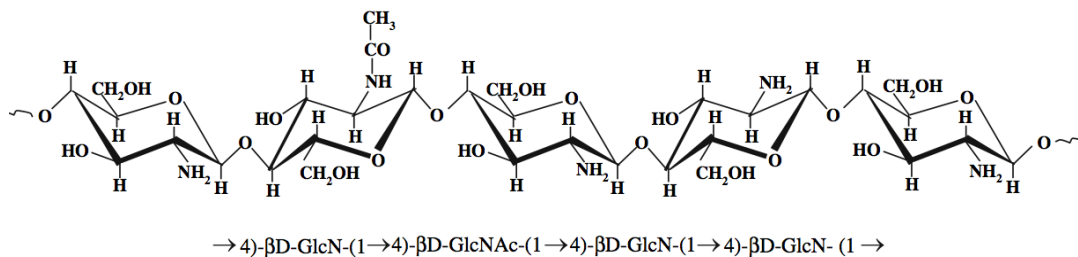


**Figure 2. Primary Structure of Chitosan [24]**

## Methods

In this project, chitosan was used as the dispersion medium for hydroxyapatite nanoparticles (HANPs) to create a novel nanocomposite. Chemo-mechanical processing in the form of ball-milling was used to make the final nanocomposite. Various chemical and physical properties of the composite were analyzed. Chemical properties of the composites were explored using energy dispersive X-ray spectroscopy (EDX) for elemental analysis and nuclear magnetic resonance spectroscopy (NMR) for functional group analysis. Physical characterization included particle size analysis using a particle analyzer and scanning electron microscopy (SEM), and phase characterization was performed using X-ray diffraction spectroscopy (XRD).

### *Composite Preparation*

HANPs were purchased from Nanoshel (Wilmington, Del.) and low molecular weight chitosan powder was purchased from Sigma Aldrich (St. Louis, Mo.). Four composites were prepared with varying fractions of HANPs and chitosan powder. Composites consisted of 10%, 30%, 50%, and 70% chitosan by weight and corresponding weight fraction of HANPs (Table 3). Each sample was prepared by mixing chitosan powder with water and 2% acetic acid. HANPs were then added and the solution was mixed for six hours at 37°C and 800rpm.

**Table 3. Weight Fractions of Prepared Composites**

| Composite | Chitosan (%wt) | HANPs (%wt) |
|-----------|----------------|-------------|
| 1         | 10             | 90          |
| 2         | 30             | 70          |
| 3         | 50             | 50          |
| 4         | 70             | 30          |

## ***Chemo-Mechanical Processing***

The goal of the study was to create a novel nanocomposite between chitosan and HANPs. Particle size analysis showed that none of the prepared composites consisted of particles within the nanometer range, thus the particle size of the composite needed to be further reduced. Because Composite 1 produced the smallest particle size, this fraction of materials was used for further particle size reduction. In order to reduce the size of the particles, chemo-mechanical processing in the form of ball-milling was performed on samples of Composite 1. A ceramic zirconia vial and ceramic zirconia balls were used in combination with a ball-mill for processing. Samples of Composite 1 were ball-milled for 36 hours to determine if particle size could be further reduced.

## **Results**

### ***Particle Size Determination***

#### **Starting Materials**

The particle size of HANPs and chitosan powder was analyzed using a laser diffraction particle size distribution analyzer (Partica LA-950, Horiba, Houston, TX) and scanning electron microscopy (SEM) (Fig. 3,4). Particle size for each sample was determined from SEM images using ImageJ software.

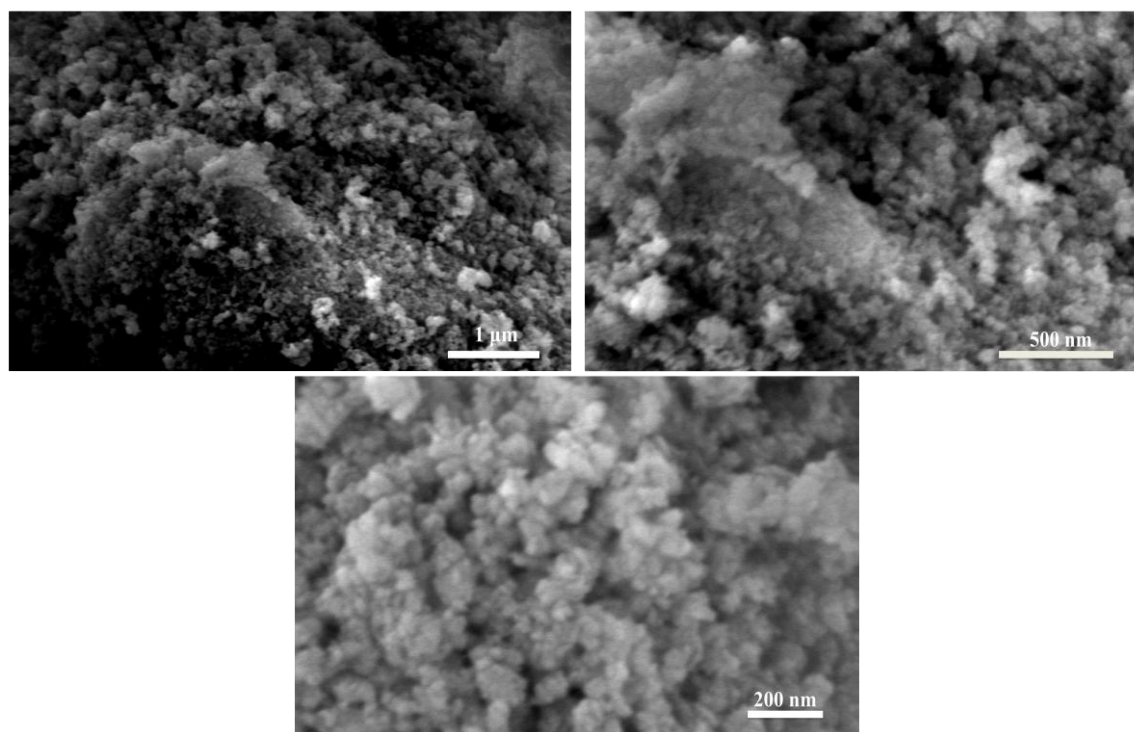


**Figure 3. SEM of Hydroxyapatite Nanoparticles**

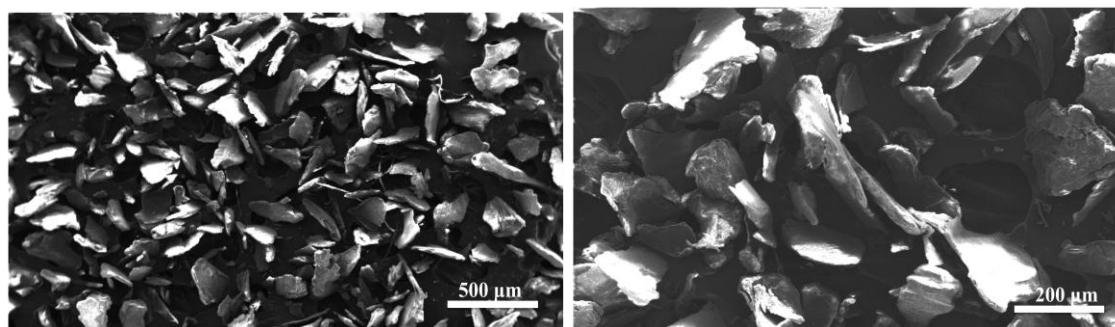


**Figure 4. SEM of Chitoan Powder**

Mean particle size of chitosan powder was determined to be 218µm with particle analyzer. Mean particle size of chitosan from SEM analysis was determined to be 204µm. Mean particle size of HANPs was determined to be 275nm with particle analyzer. Mean particle size of

HANPs from SEM analysis was determined to be 82.5nm. The inconsistency in measured data between particle size analyzer and SEM images for HANPs is believed to be associated with HANPs agglomeration in analysis with the particle analyzer. SEM images confirm that individual HANPs particles are less than 100nm.

### Composites

All four composites were analyzed through SEM (Fig. 5-8). Samples of each composite were dried before SEM analysis and coated through gold sputtering. Particle size for each composite was determined through SEM images using ImageJ software. Measurements were repeated on three different samples for each of the four composites. Each of the three samples was measured three times for a total of nine measurements for each composite (Table 4).

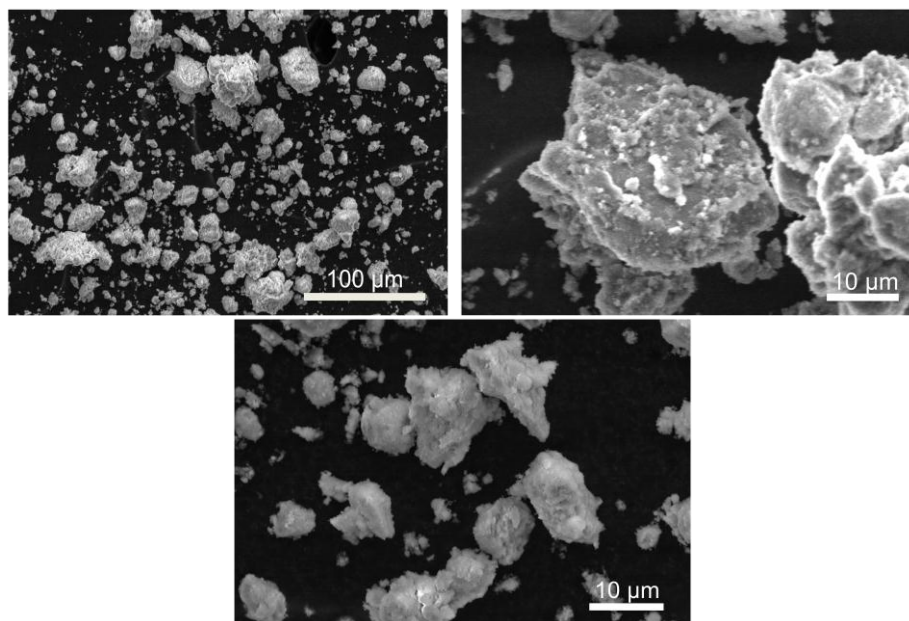


**Figure 5. SEM Composite 1**

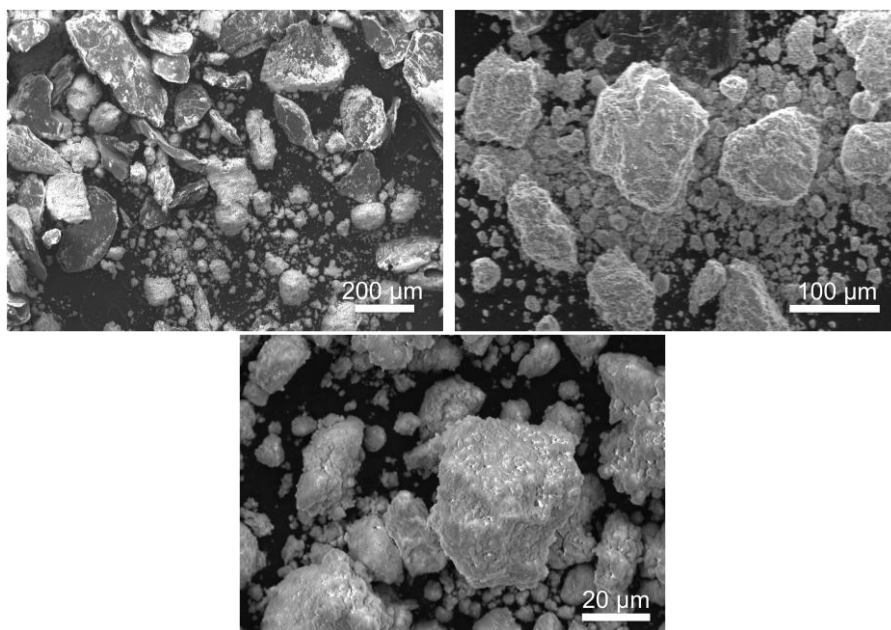


**Figure 6. SEM Composite 2**

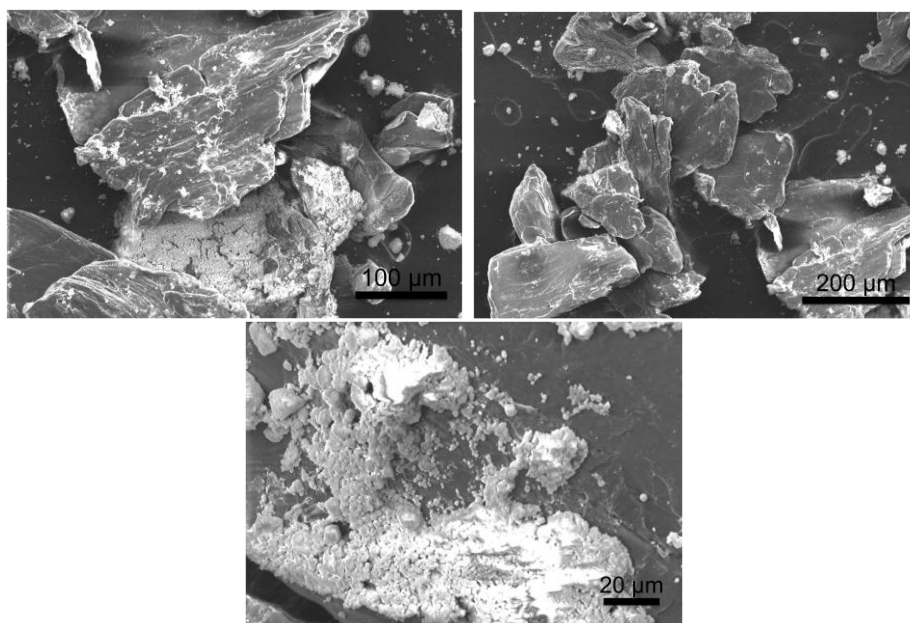


**Figure 7. SEM Composite 3**

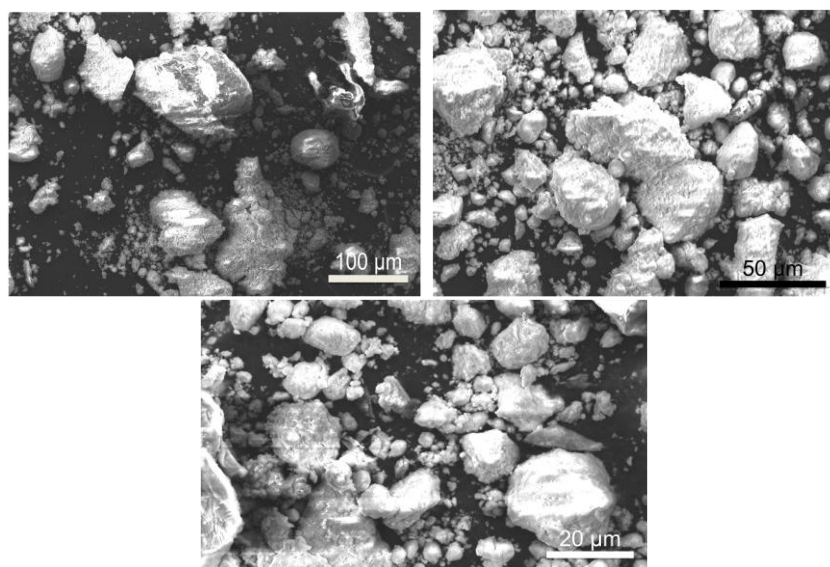


**Figure 8. SEM Composite 4**

**Table 4. Particle Size of Composites**

| Composite | Particle Size* |
|-----------|----------------|
| 1         | 15.9µm         |
| 2         | 113µm          |
| 3         | 190µm          |
| 4         | 22.0µm         |

\*Based on preliminary visual data

Particle size analysis showed that Composite 1 (90% HANPs, 10% chitosan) produced the smallest particles, however none of the composites had consistent particle size within the nanometer range.



**Chemo-Mechanical Processed Composites**

Samples of Composite 1 were ball-milled for 36 hours to determine if particle size could be further reduced. Average particle size was measured with a particle size analyzer. Results of particle size analysis for three different samples after 36 hours of ball-milling can be found in Table 5. SEM of Composite 1 after 36 hours of ball-milling can be found in Figure 9.

**Table 5. Average Particle Size of Composite 1 after Chemo-Mechanical Processing**

| <b>Composite 1 Sample</b> | <b>Initial Average Particle Size</b> | <b>Average Particle Size After Processing</b> |
|---------------------------|--------------------------------------|---|
| 1                         | 778 nm                               | 516 nm  |
| 2                         | 661 nm                               | 285 nm  |
| 3                         | 536 nm                               | 436 nm  |

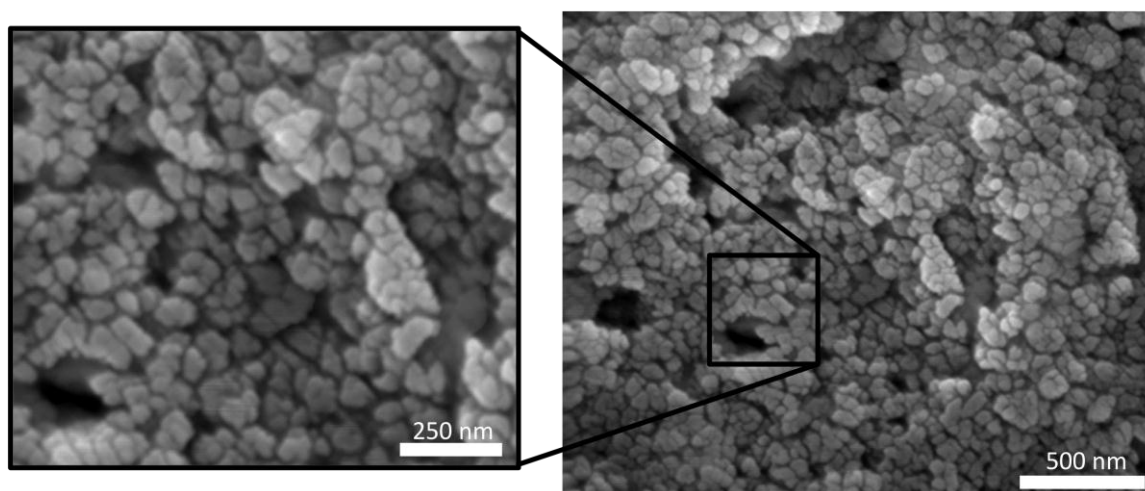


**Figure 9. SEM of Composite 1 after Chemo-Mechanical Processing**

Chemo-mechanical processing of samples through ball-milling successfully reduced the particle size of the composite. SEM images of the ball-milled composite reveal that individual particles are less than 100nm, however particles appear to be fused together.

### ***Energy Dispersion X-ray Spectroscopy (EDX)***

EDX was performed using the EDX function on a scanning electron microscope for each of the four composites. Results of EDX analysis for samples of composites can be found in Figures 10-13.

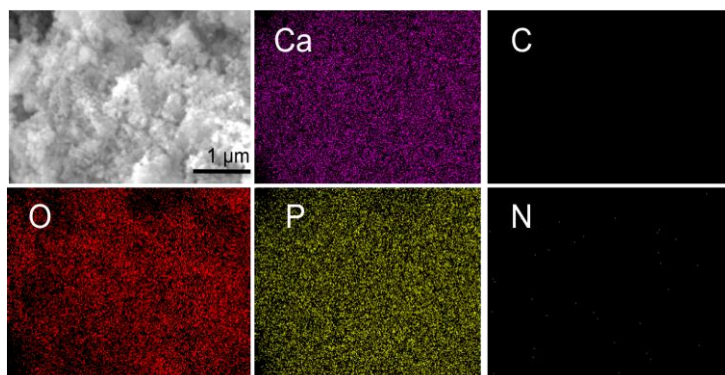


**Figure 10. EDX of Composite 1**

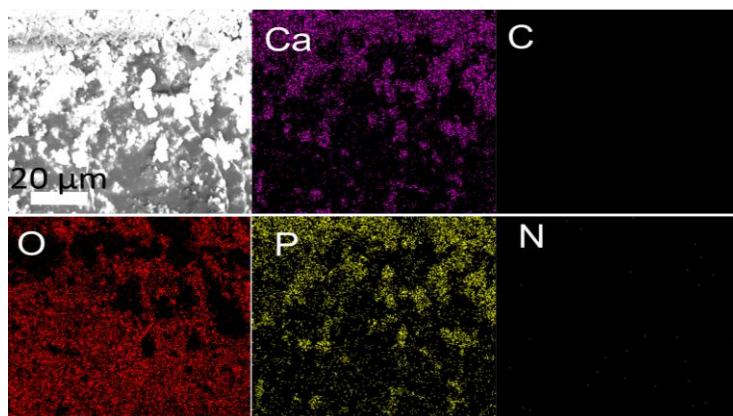


**Figure 11. EDX of Composite 2**

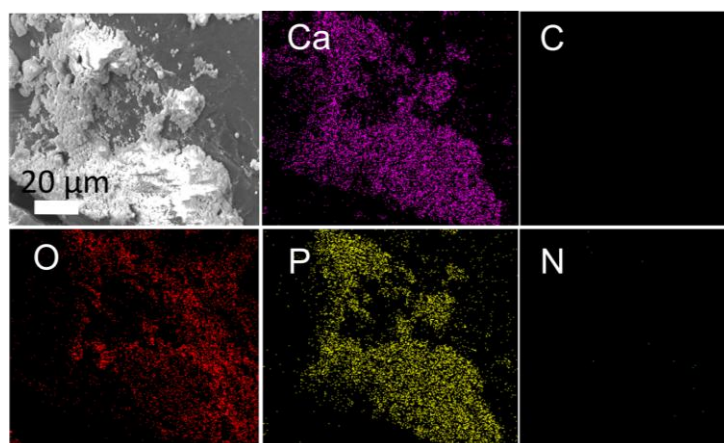


**Figure 12. EDX of Composite 3**

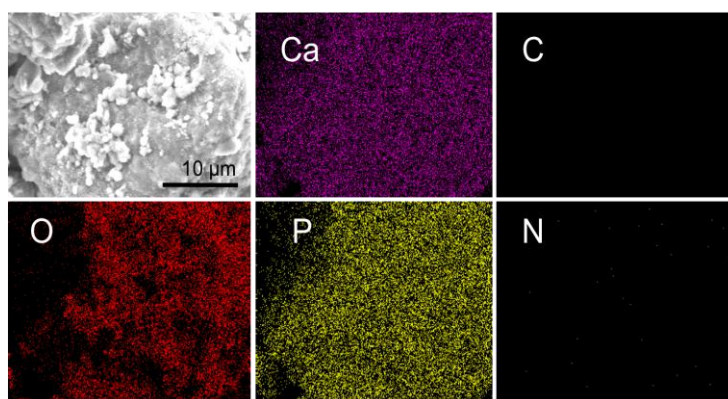


**Figure 13. EDX of Composite 4**

EDX analysis of all composites showed areas of calcium, phosphorus, and oxygen. All these elements are found in hydroxyapatite, however of these elements only oxygen is present in chitosan. Further analysis needs to be done in the future to determine if carbon and nitrogen are present in the samples and were undetected by EDX.

## ***Nuclear Magnetic Resonance Spectroscopy (NMR)***

In order to determine the functional groups present in the composites, NMR spectroscopy was performed on samples of each composite (Fig. 14-17).

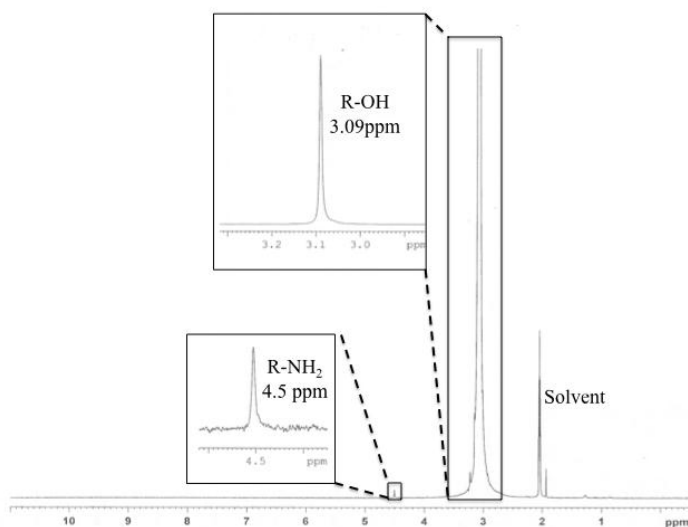


**Figure 14. NMR of Composite 1**

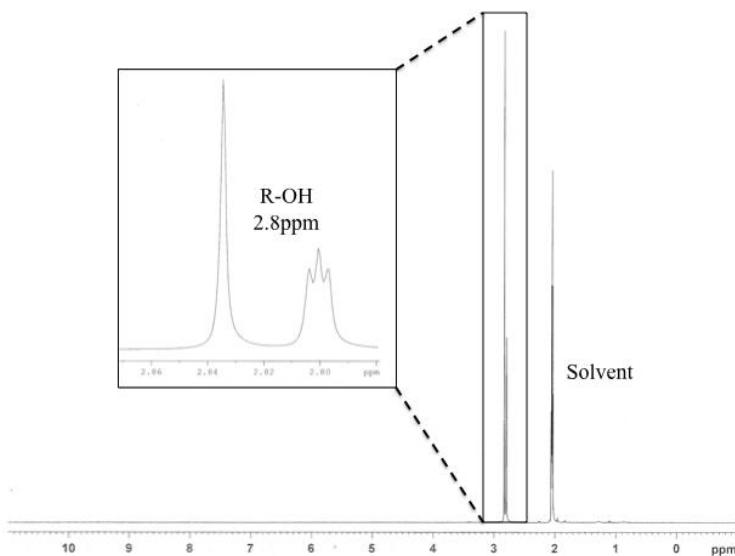


**Figure 15. NMR of Composite 2**

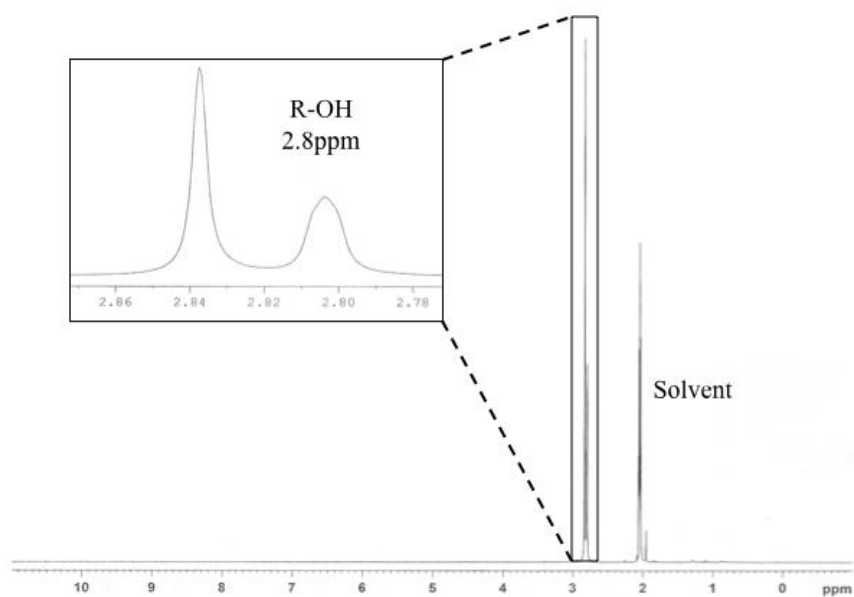


Figure 16. NMR of Composite 3

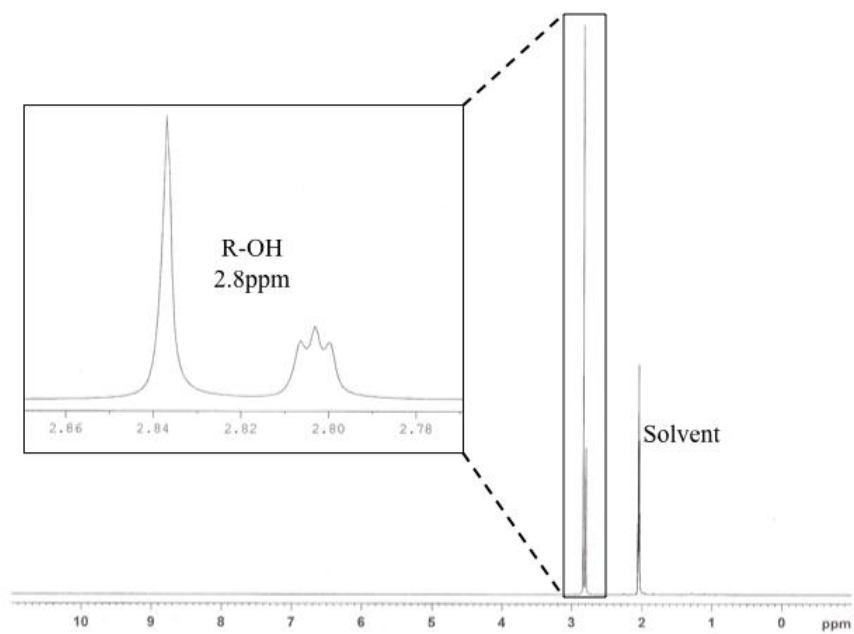
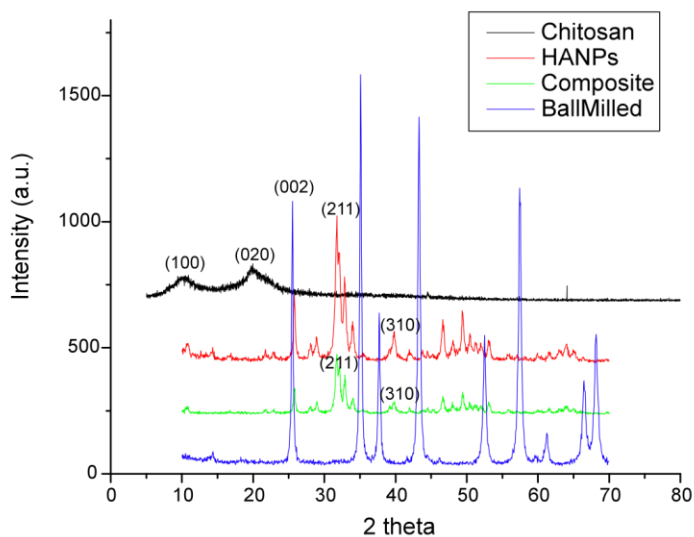


Figure 17. NMR of Composite 4

NMR revealed hydroxyl groups in each composite, however only Composite 1 showed the amine group from chitosan.

### ***X-Ray Diffraction Spectroscopy (XRD)***

To determine if phase changes occurred between the starting materials and composite, powder x-ray diffraction was performed on samples of chitosan powder, HANPs, Composite 1, and Composite 1 after 36 hours of ball-milling (Fig. 18).



**Figure 18. XRD of chitosan powder, HANPs, Composite 1, and Composite 1 after 36 hours ball-milling**

The major peaks measured for chitosan powder and HANPs, match peaks found in previous studies [25,26]. Composite 1 retained a similar crystal structure to HANPs as the XRD spectra for the two samples have nearly identical peaks. The (100) and (020) peaks found in

chitosan powder are absent in both Composite 1 and Composite 1 after ball-milling. Both Composite 1 and Composite 1 after ball-milling retained the (002) peak characteristic of HANPs [26,27]. After ball-milling the (002) peak in Composite 1 showed increased intensity. Several new peaks appeared in Composite 1 after ball-milling.

## **Discussion**

### **Particle size analysis**

Particle size analysis showed that the optimal fraction for making a chitosan-HANPs nanocomposite is 10% chitosan powder and 90% HANPs (dry weight fraction). Though none of the initial composites had particle sizes within the nanometer range, chemo-mechanical processing successfully reduced the particle size to a desired range.

### **EDX**

EDX analysis revealed that the surface of the composites was mostly composed of calcium, phosphorus, and oxygen. These results may show that hydroxyapatite is the predominant material on the surface of composite particles. Further testing of the processed materials needs to be performed to understand if the composite consists of chitosan particles coated in HANPs.

### **NMR**

NMR data showed some chemical properties of the starting materials remained distinct in the composite, including hydroxyl groups and some amine groups in Composite 1. The absence of the amine group in Composites 2-4 could be explained by the potential coordination bond

between the amine groups of chitosan and the  $\text{Ca}^{2+}$  ions of hydroxyapatite (Fig. 19). From the structure of the two materials, the particles may also be held together by hydrogen bonding, but further analysis is necessary to confirm this bonding.

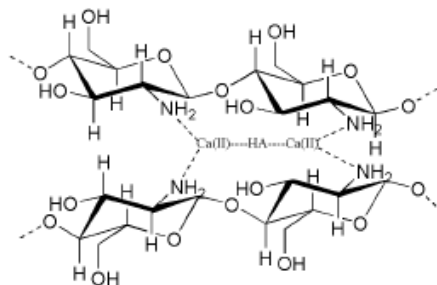


**Figure 19. Possible Coordination Bond between Hydroxyapatite and Chitosan [4]**

## XRD

XRD analysis revealed Composite 1 retained major crystal properties of HANPs both before and after chemo-mechanical processing. Several new peaks appeared after processing. Further studies are necessary to determine if these peaks represent new crystal structures, increased intensity of existing structures, or contamination by the zirconia ceramic vial and balls.

## Conclusions

It was determined through this study that the optimal fraction for making a chitosan-HANPs nanocomposite is 10% chitosan powder and 90% HANPs. Through chemo-mechanical processing the average particle size of this composite was reduced from 778nm to 285nm.

The outcomes of this project were a method for mixing chitosan powder and HANPs to make a nanocomposite. Chemical analysis through EDX and NMR showed that some of the chemical properties of the starting materials remained distinct in the composite, however there is



some evidence of a coordination bond between the amine groups of chitosan and the  $\text{Ca}^{2+}$  ions of hydroxyapatite. Analysis of composites through XRD revealed that Composite 1 retained the major crystal properties of HANPs both before and after chemo-mechanical processing, however several new peaks appeared after processing. More experiments must be conducted to confirm whether these peaks are evidence of new crystal phases, intensification of existing phases, or contamination from processing.

## **Future Directions**

### **Sample Preparation**

An ideal composite will be one in which chitosan particles and HANPs are evenly dispersed. In order to create such a composite and one with even further reduced particle size, the particle size of chitosan powder should be closer to that of HANPs. One way to achieve this would be processing the chitosan powder through chemo-mechanical processing before mixing with HANPs.

### **In vivo Studies**

Samples of Composite 1 have been sent to the University of Arkansas for Medical Sciences (UAMS) in Little Rock, Arkansas. Ernest Ferris, M.D., of the Department of Radiology, will be conducting *in vivo* studies in rabbits with the composite to determine the immune response and osseointegration of the composite.

## References

- [1] S.B. Kim, Y.J. Kim, T.L. Yoon, S.A. Park, I.H. Cho, E.J. Kim, I.A. Kim, J.-W. Shin, *Biomaterials* 25 (2004) 5715-5723.
- [2] M. Bohner, *North* 13 (2010) 24-30.
- [3] J.S. Temenoff, a G. Mikos, *Biomaterials* 21 (2000) 2405-12.
- [4] J. Venkatesan, S.-kwon Kim, *Marine Drugs* 8 (2010) 2252-2266.
- [5] S. Ozawa, S. Kasugai, *Biomaterials* 17 (1996) 23-29.
- [6] B.D. Chithrani, A. a Ghazani, W.C.W. Chan, *Nano Letters* 6 (2006) 662-8.
- [7] R. Murugan, S. Ramakrishna, *Biomaterials* 25 (2004) 3829-35.
- [8] G. Beck, S.-W. Ha, C. Camalier, T. Vikulina, M. Yamaguchi, L. Yan, J.-K. Lee, M.N. Weitzmann, *Bone* 46, Supple (2010) S16.
- [9] S.D. Perrault, W.C.W. Chan, *Proceedings of the National Academy of Sciences of the United States of America* 107 (2010) 11194-9.
- [10] F. Kratz, *Journal of Controlled Release* 132 (2008) 171-183.
- [11] A. Trapani, J. Sitterberg, U. Bakowsky, T. Kissel, *International Journal of Pharmaceutics* 375 (2009) 97-106.
- [12] R. Tan, X. Niu, S. Gan, Q. Feng, *Journal of Materials Science. Materials in Medicine* 20 (2009) 1245-53.
- [13] H. Uda, Y. Sugawara, M. Nakasu, *Journal of Plastic, Reconstructive & Aesthetic Surgery* 59 (2006) 188-196.
- [14] R. a. a. Muzzarelli, *Carbohydrate Polymers* 76 (2009) 167-182.
- [15] I. Pelin, S. Maier, G. Chitanu, *Materials Science and Engineering C* 29 (2009) 2188-2194.
- [16] S. Wang, D.H.R. Kempen, M.J. Yaszemski, L. Lu, *Biomaterials* 30 (2009) 3359-70.
- [17] M. Jayabalan, K. Shalumon, M. Mitha, K. Ganesan, *Acta Biomaterialia* 6 (2010) 763-775.
- [18] C. Deng, J. Weng, X. Lu, S. Zhou, J. Wan, *Materials Science and Engineering C* 28 (2008) 1304-1310.
- [19] J. Hao, Y. Liu, S. Zhou, Z. Li, X. Deng, *Biomaterials* 24 (2003) 1531-1539.
- [20] C. Jäger, T. Welzel, W. Meyer-Zaika, M. Epple, *Magnetic Resonance in Chemistry : MRC* 44 (2006) 573-80.
- [21] J.C. Elliott, R.M. Wilson, S.E.P. Dowker, *Advances in X-ray Analysis* 45 (2002) 172-181.
- [22] R. Jayakumar, D. Menon, K. Manzoor, S.V. Nair, H. Tamura, *Carbohydrate Polymers* 82 (2010) 227-232.
- [23] Q. Hu, *Biomaterials* 25 (2004) 779-785.
- [24] K.V. Harish Prashanth, R.N. Tharanathan, *Trends in Food Science & Technology* 18 (2007) 117-131.
- [25] Y. Zhang, J.R. Venugopal, A. El-Turki, S. Ramakrishna, B. Su, C.T. Lim, *Biomaterials* 29 (2008) 4314-22.
- [26] C. Li-yun, Z. Chuan-bo, H. Jian-feng, *Materials Letters* 59 (2005) 1902-1906.
- [27] Y.X. Pang, X. Bao, *Journal of the European Ceramic Society* 23 (2003) 1697-1704.